Search for the ^{73}Ga ground-state doublet splitting in the β decay of ^{73}Zn

V. Vedia,[1,*] V. Paziy,[1] L. M. Fraile,[1] H. Mach,[1,2,†] W. B. Walters,[3] A. Aprahamian,[4] C. Bernards,[5,6]
J. A. Briz,[7,‡] B. Bucher,[4,8] C. J. Chiara,[3,9] Z. Dlouhý,[10,§] I. Gheorghe,[11] D. Ghiţă,[11] P. Hoff,[12] J. Jolie,[13] U. Köster,[14]
W. Kurcewicz,[15] R. Lică,[11] N. Mărginean,[11] R. Mărginean,[11] B. Olaizola,[1,16] J.-M. Régis,[5] M. Rudigier,[17] T. Sava,[11]
G. S. Simpson,[18] M. Stănoiu,[11] and L. Stroe[11]

[1]*Grupo de Física Nuclear, Facultad de Ciencias Físicas, Universidad Complutense-CEI Moncloa, E-28040 Madrid, Spain*
[2]*National Centre for Nuclear Research, BP1, ul. Hoża 69, 00-681, Warsaw, Poland*
[3]*Department of Chemistry and Biochemistry, University of Maryland, College Park, Maryland 20742, USA*
[4]*Department of Physics, University of Notre Dame, Notre Dame, Indiana 46556, USA*
[5]*Institut für Kernphysik, Köln, Germany*
[6]*Wright Nuclear Structure Laboratory, Yale University, New Haven, Connecticut 06520, USA*
[7]*Instituto de Estructura de la Materia, CSIC, 28006 Madrid, Spain*
[8]*Lawrence Livermore National Laboratory, Livermore, California 94550, USA*
[9]*Physics Division, Argonne National Laboratory, Argonne, Illinois 60439, USA*
[10]*Nuclear Physics Institute of the AS CR, Řež, Czech Republic*
[11]*"Horia Hulubei" National Institute for Physics and Nuclear Engineering, Magurele, Romania*
[12]*Department of Chemistry, University of Oslo, Oslo, Norway*
[13]*Institut für Kernphysik, Universität zu Köln, Zulpicher Strasse 77, D-50937, Köln, Germany*
[14]*Institut Laue Langevin, 71 avenue des Martyrs, 38042 Grenoble Cedex 9, France*
[15]*Faculty of Physics, University of Warsaw, Pasteura 5, PL 02-93 Warsaw, Poland*
[16]*TRIUMF, 4004 Wesbrook Mall, Vancouver, BC V6T 2A3, Canada*
[17]*Department of Physics, University of Surrey, Guildford GU2 7XH, United Kingdom*
[18]*LPSC, Université Joseph Fourier Grenoble 1, CNRS/IN2P3, Institut National Polytechnique de Grenoble,
F-38026 Grenoble Cedex, France*

The existence of two close-lying nuclear states in ^{73}Ga has recently been experimentally determined: a $1/2^-$ spin-parity for the ground state was measured in a laser spectroscopy experiment, while a $J^\pi = 3/2^-$ level was observed in transfer reactions. This scenario is supported by Coulomb excitation studies, which set a limit for the energy splitting of 0.8 keV. In this work, we report on the study of the excited structure of ^{73}Ga populated in the β decay of ^{73}Zn produced at ISOLDE, CERN. Using β-gated, γ-ray singles, and γ-γ coincidences, we have searched for energy differences to try to delimit the ground-state energy splitting, providing a more stringent energy difference limit. Three new half-lives of excited states in ^{73}Ga have been measured using the fast-timing method with LaBr$_3$(Ce) detectors. From our study, we help clarify the excited structure of ^{73}Ga and we extend the existing ^{73}Zn decay to ^{73}Ga with 8 new energy levels and 35 γ transitions. We observe a 195-keV transition consistent with a γ ray de-exciting a short-lived state in the β-decay parent ^{73}Zn.

I. INTRODUCTION

The understanding of the evolution of single-particle states around shell closures and of the interplay of spherical and collective configurations in neutron-rich nuclei is a subject of great relevance in modern nuclear structure studies. The region of exotic nuclei in the $N = 40$ to $N = 50$ region is of specific interest in this context. The presence of a possible subshell closure around Ni ($Z = 28$) arising from the $N = 40$ oscillator shell has been a question of debate. The measurement of B($E2$) transition rates in neutron-rich Zn ($Z = 30$) isotopes [1] underlines the stability of the neutron $N = 50$ shell closure and

the role of polarization effects from the $Z = 28$ proton shell. Such stability has been recently challenged by experimental evidence that points towards the weakening of the $N = 50$ shell closure around ^{78}Ni and the coexistence of deformed low-lying intruder states with the normal configuration ground states [2–5].

Gallium isotopes with $Z = 31$, have only three protons outside of the $Z = 28$ shell closure, provide a good testing ground to investigate the onset of collectivity in the region and the effect of core polarization. The evolution of the ground-state spin-parity assignments of odd-Ga isotopes from ^{71}Ga to ^{81}Ga [6] shows structural modifications when moving from $N = 40$ to $N = 50$.

The study of collectivity in the $Z = 28$ region for $N > 40$ reveals that the largest B($E2$) values are measured at $N = 42$ for ^{72}Zn$_{42}$, ^{74}Ge$_{42}$, and ^{76}Se$_{42}$ [7–9]. Therefore, ^{73}Ga, with $N = 42$, is of great interest. The collectivity in this odd-Z nuclide has been known after two-neutron transfer
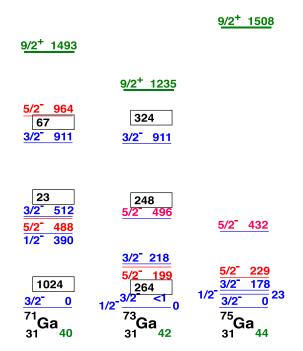
FIG. 1. Selected low-spin levels in ^{71,73,75}Ga showing the (t,p) cross sections in the rectangular boxes, along with the low energy for the g$_{9/2}$ single proton level. See text for details.

(t,p) reaction studies on stable ^{69,71}Ge [10–12]. The ^{73}Ga spectroscopic information was deduced from the transferred angular momentum. The single-proton p$_{3/2}$ strength splits about equally among three states in ^{73}Ga [10], in contrast to ^{71}Ga, where it is concentrated almost entirely in the ground state (g.s.). The apparent $l = 0$ transfer for the ^{71}Ga(t,p) reaction populating the g.s. of ^{73}Ga provided support for the assignment of $3/2^-$ spin-parity. A $3/2^-$ assignment for the ^{73}Ga ground state stems from a normal shell model ordering, with three protons occupying the πp$_{3/2}$ orbital, and it is also in accordance with the systematics of the region because both the lighter ^{67,69,71}Ga [13] and the heavier ^{75,77,79}Ga have $3/2^-$ ground states. The earlier assignment was revised by a later collinear laser spectroscopy study that measured the ^{73}Ga ground state to unambiguously have a $1/2^-$ spin-parity [6]. This is consistent with the hypothesis in Ref. [14] of $1/2^-$ and $3/2^-$ quasi-degenerate states, based on the downward shift in excitation energy of the $1/2^-$ state in the neighbours of ^{73}Ga, together with the absence of the $1/2^-$ state in ^{73}Ga at higher energies.

The features of the ^{73}Ga structure are presented in Fig. 1 together with the location of the $9/2^+$ single-proton state reported by Stefanescu *et al.* [14]. At about the same time, Coulomb excitation was employed by Diriken *et al.* [15] to study collectivity in ^{73}Ga. Their results provided evidence for the $1/2^-$-$3/2^-$ doublet close to the ground state with an energy splitting below 0.8 keV. This fact shows the exotic character of the first excited $3/2^-$ in ^{73}Ga, since typical nuclear excitation energies are 10^2 to 10^4 times larger and there are very few isotopes among the whole nuclear landscape with excited states in the eV energy range [16–18].

In addition to investigating the ground-state doublet splitting, the interest in studying the β decay of ^{73}Zn to ^{73}Ga resides also in understanding the unclear situation of the ^{73}Zn parent, where an isomeric state at 195.5 keV has been reported with conflicting half-lifes of 5.8 s by Runte *et al.* [19] (de-excited by 195.5 and 42 keV γ rays) and of 13 ms by Huhta *et al.* [20]. In addition, a 199-keV transition with a half-life of 3.9 s reported in Ref. [21], and consistent with the ^{73}Cu β-decay half-life, could not be confirmed in Ref. [20].

To provide further insight into ^{73}Ga we have studied the level structure populated in the β decay of ^{73}Zn produced at ISOLDE, CERN, and used the data to attempt to determine the separation between the two low-energy levels. The spin and parity of the parent ^{73}Zn is proposed as $(1/2^-)$ [22], hence direct β decay will only be allowed to spin $1/2^-$ and $3/2^-$ levels. We use γ-ray spectroscopy to clarify and extend the known level scheme and the Advanced Time Delayed $\beta\gamma\gamma$(t) method [23,24] to measure excited level lifetimes and deduce transition probabilities to help understand the structure of ^{73}Ga.

II. EXPERIMENTAL DETAILS

Data from this work were measured during the IS441 experiment at the ISOLDE-CERN facility [25], being a part of a wider investigation of the nuclear structure of the isotopes $^{73-82}$Ga populated in the β decay of Zn nuclei [26,27]. In this investigation, we took advantage of the high purity of the Zn beams at ISOLDE. The zinc atoms were produced by the collision of 1.4 GeV protons on the neutron converter [28] of a UC$_x$ target unit that was operated at $\sim$2 000°C to optimize the zinc release. The target was equipped with a special quartz transfer line [29,30] to block the release of contaminants, and with the ISOLDE Resonance Ionization Laser Ion Source (RILIS) [31] for selective ionization of Zn. The ionized isotopes of interest were accelerated by a 30-kV extraction potential and guided through a magnetic high-resolution mass separator (HRS) with a resolving power of $\Delta M/M \sim 5000$ where mass $A = 73$ ions were selected.

The beam was transported to the center of the experimental setup where it was collected on an aluminum foil. Due to the high production rate of ^{73}Zn together with its long half-life, the beam was collected during 1 s after the impact of a proton pulse on the target, with an average intensity of 3×10^{13} protons. The activity was afterwards left to decay away for about two half-lives, matching the time to a supercycle—the time structure in which the proton pulses are organized in the CERN accelerator complex—which in our experiment varied from 38 to 39 or 40 proton pulses, the pulses being interspaced 1.2 s, for a total of 45.6, 46.8, or 48.0 s.

The experimental setup consisted of two HPGe detectors, which were used for γ-ray identification and the coincidence study, an ultrafast 3-mm-thick NE111A plastic scintillator, which was used as β detector, and two LaBr$_3$(Ce) crystals with the shape of truncated cones that were used for lifetime measurements together with the β plastic. The scintillators were coupled to fast photomultiplier tubes (PMTs), equipped with two output signals, the anode (negative) and the dynode (positive). The energy information was taken from the dynode output of the PMTs, the signals were preamplified and digitized

TABLE I. Most intense γ-ray energies used for the calibration of the HPGe detectors [22,33–35].

Energy (keV)	Parent nucleus	Energy (keV)	Parent nucleus
53.45 *5*	^{73}Ga	778.9040 *18*	^{152}Eu
121.7817 *3*	^{152}Eu	964.079 *18*	^{152}Eu
162.660 *1*	^{140}Ba	1120.294 *6*	^{214}Bi
244.6975 *8*	^{152}Eu	1065.1 *1*	^{73}Ga
297.32 *5*	^{73}Ga	1299.14 *9*	^{152}Eu
325.70 *7*	^{73}Ga	1408.006 *3*	^{152}Eu
423.722 *1*	^{140}Ba	1596.21 *4*	^{140}Ba
547.001 *5*	^{138}Cs	2521.40 *5*	^{140}Ba
583.187 *2*	^{208}Tl	2731.12 *15*	^{138}Cs
609.320 *5*	^{214}Bi	3339.01 *25*	^{138}Cs

in a digital data acquisition system Pixie-4 composed by four Digital Gamma Finder cards [32], together with the energy signals from the HPGe detectors. The timing information was extracted from the anode signals of the PMTs of the NE111A and LaBr$_3$(Ce) detectors. First, they were processed by an ORTEC 935 Constant Fraction Discriminator and afterwards fed into an ORTEC 567 Time to Amplitude Converter (TAC) to provide the time difference between the β detector, which acted as the start signal, and the LaBr$_3$(Ce) signals, used as the stop. An additional TAC started and stopped by LaBr$_3$(Ce) signals was also set up. The TAC output signals were digitized in the Pixie-4 system. Logic signals were also included in the data acquisition, including the time of proton impact on target, which made it possible to correlate the activity with the instant of production. Data were recorded independently and sorted off-line with custom software before analysis.

Due to the small separation between the $1/2^-$ and the $3/2^-$ states, special attention was paid to the energy calibration of the HPGe detectors. Calibration functions were built using γ-ray sources of ^{152}Eu, ^{138}Cs, ^{140}Ba, the well-known γ rays in the ^{73}Ge β-decay daughter, and γ-ray from the natural background. Table I presents γ-ray energies used for the calibration of the HPGe detectors. The calibration function reproduces very well the energy values in the range from a few keV to 3 MeV, and allows us to calculate energy differences between γ-cascades with an estimated precision below 0.2 keV.

In addition to the spectroscopic information, in this work we made use of the Advanced Time-Delayed method (ATD) $\beta\gamma\gamma$(t) method [23,24,36] to measure lifetimes of the excited states in ^{73}Ga, which provided access to the reduced transition probabilities. This electronic timing method employs the high-resolution HPGe detectors for branch selection and the fast scintillators for timing measurements as described above. When the lifetime is in the range of hundreds of picoseconds to a few nanoseconds the time distribution in the TAC spectrum is a combination of a quasi-Gaussian response function plus an exponential decay that can be deconvoluted to extract the half-life. Shorter lifetimes are derived from the shift of the centroid position of the time distribution. The latter procedure requires precise calibrations of the time response of the LaBr$_3$(Ce) detectors, both for full-energy and for Compton events. The

Full Energy peak (FEP) curve provides the time response of the system measured at different photopeak energies. In this work, the FEP curve was obtained by using prompt transitions from the ^{140}Ba/^{140}La and ^{138}Cs/^{138}Ba sources. The Compton curve was calculated by Compton events from selected γ transitions in ^{140}Ce. Additionally, the very small time walk of the β detector was taken care of by an event-by-event correction. Further details on the calibration procedures and lifetime measurements can be found, for instance, in Refs. [27,37].

III. EXPERIMENTAL RESULTS

Singles and β-gated HPGe spectra of ^{73}Ga are shown in Fig. 2. To reduce short-lived components arising from neutron-induced reactions in the detectors and surrounding materials, a condition is imposed on the time after proton impact on the target. For our analysis we require a time window from 100 to 42 000 ms after proton impact. A further coincidence with the detection of a β signal is also requested to suppress γ-ray background, as illustrated in the b plot of Fig. 2. In addition to the neutron-induced γ transitions, it is apparent that the γ ray at 195 keV mostly disappears when these two conditions are set (see inset in the a plot of Fig. 2). This fact points to a short-lived component in the tens of ms range that does not follow the ^{73}Zn β-decay half-life.

A. Identification of γ rays and the β-decay half-life of ^{73}Zn

After the proton impact on the ISOLDE target, the ^{73}Zn beam was transported and implanted into our collection point for 1 s. During this time the activity followed the release from the target (dominated by an exponential growth) and the β decay of ^{73}Zn. After 1 s the beam implantation was blocked and the ions were left to decay until the arrival of the next proton on target. New γ rays belonging to the decay of ^{73}Zn to ^{73}Ga were identified based on their decay pattern, matching the known ^{73}Zn β-decay half-life, and using γ-γ coincidences with previously established transitions. Figure 3 illustrates the decay curves with respect to time of proton impact for the most intense γ rays of 217.4, 495.6, and 910.6 keV.

They were fitted to an exponential function yielding a ^{73}Zn half-life of 24.5 ± 0.2 s, which is in agreement with the literature value of 23.5 ± 1.0 s reported by Runte *et al.* [21]. The value and the uncertainty were obtained from the weighted average of the individual results for the most intense γ rays in the decay. To account for systematic uncertainties, and for the fact that the fit only spans two ^{73}Zn half-lives, the error has been doubled.

B. Search for isomers in the $A = 73$ chain

With the aforementioned procedure it was possible to search for γ rays with different decay half-lives. In their work [19], Runte *et al.* report a 5.8-s isomer in the $A = 73$ decay chain identified by the observation of 195.5- and 42-keV γ rays, that they assign to ^{73m}Zn, with the 42-keV γ ray connecting the levels in ^{73}Ga at 952.4 keV (known from reactions but not populated in the β decay of ^{73g}Zn) and 910.6 keV (observed in the β decay of ^{73g}Zn). Contrary to this observation, Huhta and coworkers [20] identified a much shorter lived 195.5(2)-keV γ
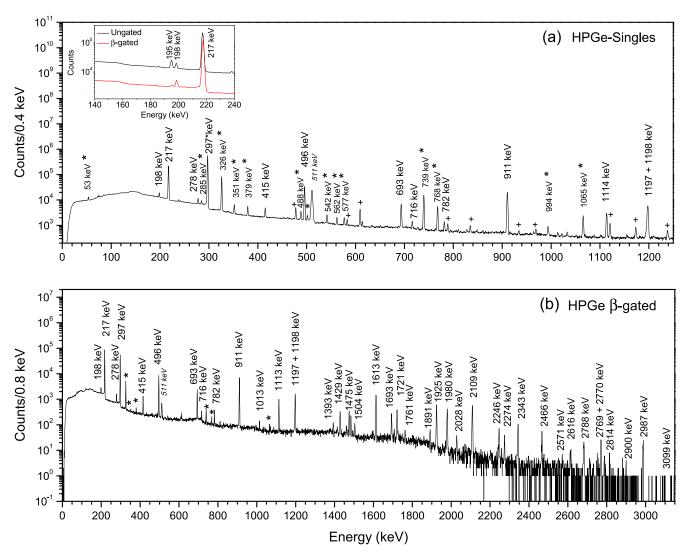
FIG. 2. Singles HPGe spectrum (a) with a time window from 100 to 42 000 ms after the proton impact. The most intense transitions in ^{73}Ga are labeled with their energy. Transitions marked with an asterisk after their energy belong to the β decay of ^{73}Ga to ^{73}Ge. γ rays marked with a cross correspond to background and contaminants. The 297 keV peak belongs to both ^{73}Ga and ^{73}Ge. The inset zooms into the low energy region with no time window and with a condition on the detection of β particles, the 195 keV γ ray mostly disappears when applying this condition. A β-gated HPGe spectrum is shown in b. The time window is the same as the one in a and the γ transitions present in ^{73}Ge are also marked with an asterisk.

transition with $T_{1/2} = 13.0(2)$ ms, de-exciting an excited state in ^{73}Zn of the same energy, with a proposed $5/2^+$ spin-parity based on the *M2* character of the transition.

In our study we observed a γ ray at 195.0 keV that decays shortly after the proton impact on target. Figure 4 shows the 195.0-keV decay curve, which overlaps with the implantation time of 1 s. The curve can be fitted to the release from the target using an exponential decay plus constant background function. The fast release constant was obtained from the time behavior of the most intense γ rays from the ^{73}Zn decay in a time window of 1000 ms, assuming a simple rise time component [38]. The fit yielded $T_{1/2} = 13.1 \pm 1.8$ ms, in agreement with the more precise literature value [20]. It should be pointed out that our result may not be very accurate due to the overlap of 13.0(2) ms with the release profile and the

dependence of the value on the fitting region. We conclude that ^{73}Zn nuclei were produced and extracted both in the ground state and in the first excited state, which decays by a 195.0-keV transition. This is in agreement with [20] and at odds with the long-lived ^{73m}Zn β-decaying isomer proposed in Ref. [19].

We found no evidence for a 42-keV γ ray neither in our singles nor β-gated HPGe spectrum; see Fig. 2. Furthermore, the γ-γ coincidences with the 910.6-keV transition showed no 42-keV γ rays. In addition, there was no hint of a 952-keV γ line in our β-gated spectrum. Thus, we exclude the presence of this 42-keV transition in the decay of ^{73}Zn to ^{73}Ga.

No indication was found in our β-γ coincidences data for a long-lived 198-keV transition ($T_{1/2} = 3.9$ s) as reported in Ref. [21], which was not found in Ref. [20] either. The 198-keV
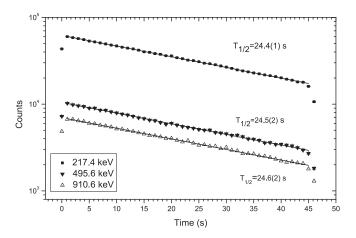
FIG. 3. Decay curves from the 217.4, 495.6, and 910.6 keV γ rays. Curves are well fitted to a single exponential component in the time range from 1 to 44 s. The half-life of 24.5 ± 0.2 s is obtained from the weighted average from the most intense γ rays and the error is corrected for estimated systematic uncertainties.

transition is consistent with belonging to the β decay of ^{73}Zn to ^{73}Ga, both in terms of its decay pattern and γ-γ coincidences.

C. Nuclear structure of ^{73}Ga

Making use of the coincidences present at the γ-γ and β-γ data sets with a time window of 100 to 42 000 ms from the proton impact, we have identified new γ rays from the β decay of ^{73}Zn. Figure 5 shows γ lines coincident with the strongest 217.4-keV transition. We have greatly extended the ^{73}Ga level scheme with 35 new γ-ray transitions and 8 new energy levels not observed previously in β-decay studies [19,21]. A summary of the γ transitions is provided in Table II. Figure 6 presents the ^{73}Ga level scheme with the new information in red. The transitions marked with a dashed line were seen in γ-γ coincidence but with very low intensity. We establish energy levels at 1113.7, 1392.7, 1721.2, 1979.6, 2245.9, 2466.1, and 2769.8 keV, whose excitation energies are in agreement with some of the levels reported by Vergnes and coworkers in
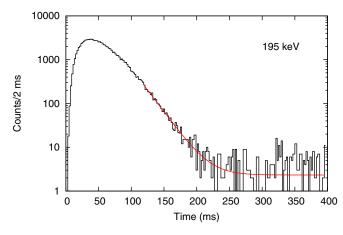

FIG. 4. Decay curve for 195.0-keV γ rays together with the fit to the release and an exponential decay component displayed in red.

transfer reactions studies [10–12]. Nonetheless, the level at 1800(3) keV identified as $3/2^-$ in the (t,p) reaction is not observed in the β decay, contrary to what could be expected from the $(1/2^-)$ ^{73}Zn ground-state decay. In our data set we also observe a 2343.6-keV γ ray, which is not placed at the level scheme but due to its decay time behavior, it clearly belongs to ^{73}Ga.

Most of the newly reported levels in this work are placed above 2 MeV in energy. Considering the $1/2^-$ spin-parity assignment for the ^{73}Zn ground state, and the fact that in our data we do not observe states with spins higher than $5/2$, this points toward $1/2^-$ and $3/2^-$ states located at energies higher than 2 MeV. This has not been previously observed in any experiment nor calculated by the available theoretical calculations [6,39]. No indirect population to the $7/2^-$ levels at 651.2 and 952.4 keV suggested in Ref. [14] is observed in the β-decay scheme.

The apparent β feeding to the states in ^{73}Ga has been calculated from the γ intensity balance between the populating and the de-exciting transitions. The ground-state feeding has been obtained making use of the absolute intensities of the most intense transitions in ^{73}Ge populated in the β decay of ^{73}Ga (325.7, 739.4, and 767.8 keV), available in the literature [22]. Due to the fact that the measuring time was not long enough to allow for all the implanted ^{73}Ga nuclei to decay away, our implanted $A = 73$ source is not in saturation and we had to calculate the fraction of ^{73}Ge in the foil. Since fresh ^{73}Zn nuclei are implanted with the arrival of every proton pulse, we have calculated the fraction of ^{73}Ge for each of them by making use of observed ^{73}Zn activity from the data and the Bateman equations, using the β-decay half-life of ^{73}Ga from literature [22]. We used the number of incoming proton pulses together with their arrival time and the time elapsed between them. With this procedure, we obtained a combined β feeding to the $1/2^-$ ground state and to the $3/2^-$ first excited state of 87(3)%. This result perfectly matches the literature value of 89% [21]. The strong β feeding from the ^{73}Zn parent to the ground-state doublet in ^{73}Ga supports the proposed $1/2^-$ spin for the ^{73}Zn ground state. Once the g.s. β feeding is obtained, the β feeding and log ft values were calculated for all levels in ^{73}Ga; they are shown in Fig. 6. They should be taken with caution since the presence of missed high-energy γ rays cannot be excluded. In particular, no β feeding from the $1/2^-$ ^{73}Zn ground state can be expected to the $5/2^-$ states in ^{73}Ga via second forbidden transitions.

D. The ground-state doublet energy splitting

To search for the energy splitting of the close-lying $1/2^-$ and $3/2^-$ states the first approach consisted of searching for energy differences between γ cascades that de-excite the same energy level, but proceed through distinct paths that include the ground and the first excited states. As an example, we consider the 910.7 keV level, where we can derive the energy separation by comparing the 693.4- to 217.4-keV and 415.2- to 297.3- to 198.4-keV cascades. In the latter case, the 198.4-keV level with a $5/2^-$ spin-parity should mainly decay to the first excited $3/2^-$ state via a predominant $M1$ transition, while the 217.4-keV state possessing spin $3/2^-$ would decay to both
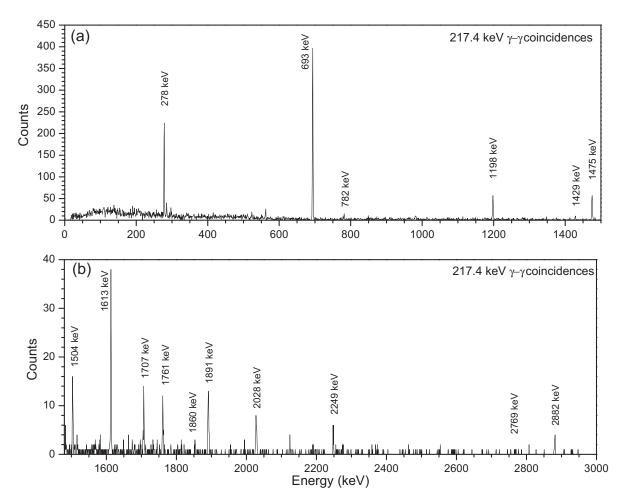
FIG. 5. Coincident γ-γ energy spectrum gated on the 217.4-keV transition. The most intense coincident peaks are labeled.

$1/2^-$ and $3/2^-$ levels, with the $1/2^-$ state being preferred in analogy with transitions in ^{75}Ga [40]. The energy splitting from this cascade is $\Delta E = -0.1 \pm 0.3$ keV, with the experimental resolution larger than the calculated difference. This is also the case for most of the combinations that we have analyzed for the ^{73}Ga energy levels, such as the 495.6-keV level decay via the 297.3- to 198.4-keV and 277.8- to 217.4-keV cascades. From the average of the γ-ray decay paths considering the information given in Table II and Fig. 6 we obtain an upper limit for the energy splitting of 0.3 keV, mainly arising from the energy resolution defined by the energy calibration described in section II.

The second approach consisted of searching for doublets in the HPGe energy spectra. Taking into account the $1/2^-$–$3/2^-$ configurations of the g.s. doublet, γ transitions that de-excite $3/2^-$ levels such as those at 2109, 911, or 217 keV, are thought to feed both states, and therefore they should appear broadened in the energy spectrum.

Hence, a systematic evaluation of peak FWHMs as a function of energy was performed. Figure 7 illustrates the relation between peak width and energy. The circles correspond to γ rays from the calibration sources of ^{152}Eu and ^{138}Cs, which are peaks with a single component, while squares represent the γ rays from the ^{73}Zn decay. Apart from the known 1194-1197-1198 triplet, the rest of the peaks follow the same

trend as the calibration sources without any visible sign of broadening. Thus, the energy separation is in the same range as the statistical fluctuations that appear in a single peak. The inset in the upper left corner of Fig. 7 zooms in the energy region from 0 to 1100 keV to get a better view of the transitions that may feed both states.

From both approaches, we conclude that the energy separation between the $1/2^-$–$3/2^-$ low-lying states is less than 0.3 keV.

E. Half lives of the excited states in ^{73}Ga

The transition rates may aid with the interpretation of the structure of ^{73}Ga and disentangle the transitions to the ground-state doublet. Therefore, we have used the ATD method [23,24,36] to measure lifetimes of the excited states in ^{73}Ga. After inspection of the β-γ time-delayed spectra, no decay slopes were identified and therefore all lifetimes assessed in this work are only accessible through the centroid shift method [36], making use of the triple $\beta\gamma\gamma(t)$ coincident fast-timing data. The levels at 217.4 and 495.6 keV are good candidates for states with measurable lifetime, since both are de-excited and populated by intense γ rays that can be selected in the LaBr$_3$(Ce) detectors. Figure 8 illustrates the LaBr$_3$(Ce) energy spectrum compared to the high resolution γ spectrum

TABLE II. All ^{73}Ga γ transitions observed in the ^{73}Zn decay with their relative intensities

E_γ (keV)	E_{initial} (keV)	E_{final} (keV)	$I_\gamma^{\text{rel a}}$ (%)	Strongest γ-γ
198.42	198.42	0[b]	2.82	297, 1194, 1494, 1726, 2571, 2788
217.42	217.41	0[b]	1005	278, 693,1197, 1475, 1891, 2249, 2769
277.9[c]3	495.62	217.41	2.1[c]3	217, 415, 1197, 1613, 1971, 2274
297.3[c]2	495.62	198.42	0.2[c]1	198, 415, 1197, 1429, 1484, 1613, 1971, 2274
415.22	910.72	495.62	2.31	217, 278, 297, 496, 782, 811, 1198
482.22	1392.73	910.72	0.11	415, 587, 693, 716, 911, 1594
495.61	495.62	0[b]	28.414	415, 1197, 1429, 1484, 1613
579.33	1692.63	1113.72	0.11	1114
586.65	1979.63	1392.73	0.11	1194, 1393
608.45	1721.23	1113.72	0.11	1114
693.41	910.72	217.41	7.74	217, 496, 1013,1198
716.12	2108.83	1392.73	0.81	1194, 1393
781.72	1692.63	910.72	1.01	415, 693, 911
810.54	1721.23	910.72	0.31	415, 693, 911
910.61	910.72	0[b]	31.616	217, 496, 1013, 1070, 1198, 1860
1013.44	1924.43	910.72	0.31	415, 496, 693, 911
1069.73	1979.64	910.72	0.21	415, 496, 693, 911
1113.62	1113.72	0[b]	5.34	1873
1194.2[c]4	1392.73	198.42	0.2[c]1	198, 587, 716, 1594
1196.9[c]3	1692.63	495.62	5.4[c]8	278, 297, 496
1198.1[c]4	2108.793	910.72	11.9[c]23	415, 693, 911
1392.93	1392.73	0[b]	0.91	587, 716, 1593
1428.72	1924.43	495.62	2.92	278, 297, 496
1475.22	1692.63	217.41	2.62	217
1483.93	1979.64	495.62	1.82	217, 278, 297, 496
1493.56	1692.63	198.42	0.11	198
1504.03	1721.23	217.41	0.61	217
1593.75	2986.65	1392.73	0.21	482 1194, 1393
1613.12	2108.83	495.62	16.313	278, 297, 496
1692.82	1692.63	0[b]	2.62	—
1707.04	1924.43	217.41	0.31	217
1721.32	1721.23	0[b]	3.23	
1726.04	1924.43	198.42	0.11	
1761.6[c]5	1979.64	217.41	0.6[c]2	
1859.53	2769.83	910.72	0.31	
1873.05	2986.65	1113.72	0.31	
1891.35	2108.83	217.41	0.81	
1924.52	1924.43	0[b]	8.17	
1970.57	2466.15	495.62	0.21	
1979.72	1979.64	0[b]	6.25	
2028.35	2245.94	217.41	0.41	217
2108.92	2108.83	0[b]	9.58	—
2246.13	2245.94	0[b]	1.12	—
2248.6[c]5	2466.15	217.41	0.3[c]1	217
2274.33	2769.83	495.62	1.11	496

TABLE II. (*Continued.*)

E_γ (keV)	E_{initial} (keV)	E_{final} (keV)	$I_\gamma^{\text{rel a}}$ (%)	Strongest γ-γ
2343.6[d]*3*			2.42	—
2466.43	2466.1*5*	0[b]	0.2*1*	—
2571.27	2769.8*3*	198.4*2*	0.1*1*	198
2616.15	2814.3*5*	198.4*2*	0.1*1*	198
2769.3[c]*5*	2986.6*5*	217.4*1*	0.2[c]*1*	217
2770.23	2769.8*3*	0[b]	1.4[c]*3*	—
2787.94	2986.6*5*	198.4*2*	0.4*1*	198
2814.25	2814.3*5*	0[b]	0.2*1*	—
2881.7[c]*5*	3098.8*5*	217.4*1*	0.1[c]*1*	217
2900.25	3098.8*5*	198.4*2*	0.2*1*	198
2986.7 3	2986.6*5*	0[b]	1.92	—
3098.86	3098.8*5*	0[b]	0.2*1*	—

[a]For absolute intensity per 100 β decays, multiply by 0.056.
[b]We refer to both states at the ground-state doublet.
[c]Obtained from coincidences.
[d]Not placed in the level scheme.

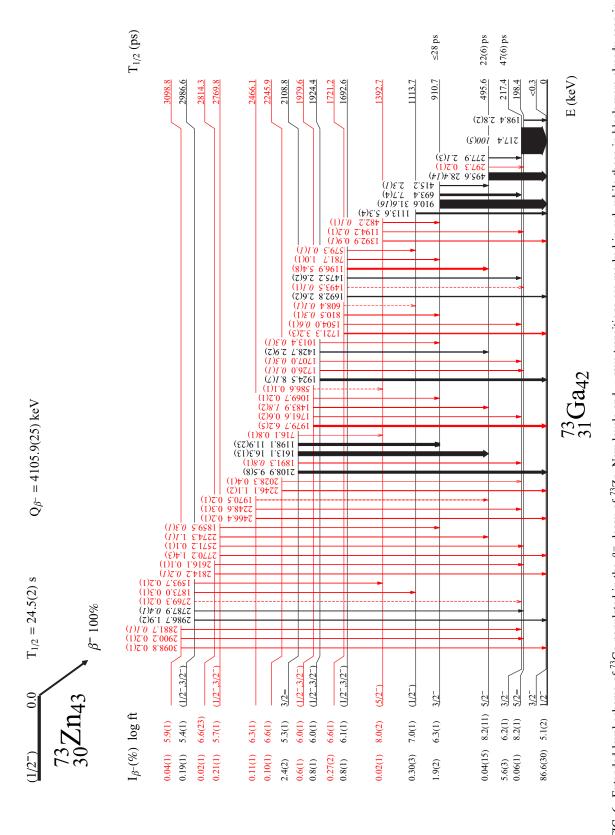from the HPGe. In addition, we also provide an upper limit for the 910.7-keV lifetime.

For the 217.4-keV state, we have extracted the $\beta\gamma\gamma$(t) information through the sequential 217.4- and 693.4-keV transitions. First, the 693.4-keV γ ray was selected in the HPGe, while the 217.4-keV full energy peak (FEP) was selected in the LaBr$_3$(Ce) spectrum (see Fig. 9). The centroid position of the time distribution with both conditions is given by $\tau_1 = \tau_0^{217} + \tau_{217} + \tau_{693} + \tau_{\text{feed}}^{911}$, where τ_0^{217} is the (prompt) time response of the setup for a FEP of 217.4 keV and τ_{feed}^{911} is the time contribution of the feeding levels. Second, the gates were reversed, with the 693.4-keV FEP selected in the LaBr$_3$(Ce) spectrum and the 217.4-keV γ ray gated on the HPGe detector. In this case, the centroid position of the time distribution is given by $\tau_2 = \tau_0^{693} + \tau_{693} + \tau_{\text{feed}}^{911}$. The mean life of the 217-keV state is obtained from $\tau_2 - \tau_1 = \tau_{217} + (\tau_0^{693} - \tau_0^{217})$. The time shifts arising from the Compton background under FEP peaks in the LaBr$_3$(Ce) detectors were corrected with the aid of the Compton curve. The system response τ_0 as a function of energy was obtained from the FEP prompt calibration curve (Sec. II), which is illustrated in Fig. 10 for one of the LaBr$_3$(Ce) detectors. In the plot the centroid positions of τ_1 and τ_2 are also shown; both centroids have been shifted by the same amount so that the τ_2 position matches the FEP curve at 693 keV, obtained by interpolation from the calibration points. The 217-keV level lifetime is then measured from the time shift of τ_1 to the calibration curve. We should underline the good agreement between the two LaBr$_3$(Ce) detectors, with τ values of 66 ± 14 ps and 68 ± 12 ps for each of them. As a final value, we take a weighted average, yielding $\tau_{217} = 67 \pm 9$ ps, which corresponds to $T_{1/2} = 47 \pm 6$ ps.

The 495.6-keV level half-life was obtained from triple $\beta\gamma\gamma$(t) coincidences with the same procedure described above, but selecting this time the 495.6- and 1613.1-keV γ transitions. The HPGe gating made it possible to eliminate the influence of 511-keV γ rays. We measured a lifetime of $\tau_{496} = 32 \pm 9$ ps, thus a half-life of $T_{1/2} = 22 \pm 6$ ps.

Concerning the 910.7-keV level, the available γ cascades are less intense than for the 217.4- and 495.6-keV states, and consequently we can only provide an upper limit of $\tau \leqslant 40$ ps. This value has been measured with the centroid shift method. For the important 198.4-keV level the scarce statistics do not allow a $\beta\gamma\gamma$ analysis to be performed, and we can only use the $\beta\gamma$ time-delayed spectra to establish a conservative limit from the nonobservation of a slope in the delayed part, which is of the order of $\tau \lesssim 60$ ps.

IV. DISCUSSION

Jiang *et al.* [41] have used the nucleon pair approximation (NPA) in the SDG-pair subspace to calculate the low-lying level scheme, the electric quadrupole and magnetic dipole moments, and $E2$ and $M1$ transition rates in ^{73}Ga, taking ^{78}Ni as a closed core. In turn, Cheal *et al.* [6] performed shell model calculations with two different interactions, JUN45 and jj44b, in a model space that uses ^{56}Ni as a core, and a $pf_{5/2} g_{9/2}$ as model space. Both calculations reproduce the presence of the two low-lying $1/2^-$ and $3/2^-$ states, and the NPA calculations find the $1/2^-$ level as the g.s. Although we have expanded the level scheme of ^{73}Ga populated in the β decay of ^{73}Zn, a comparison to the calculated energies did not provide further information, except the possible identification of some $5/2^-$ and $3/2^-$ experimental states above 1 MeV, by comparison to Ref. [41].

From the measurement of the level lifetimes and the branching ratios, transition rates were calculated. An overview is given in Table III. Using the jj44b interaction mentioned above, we have performed shell-model calculations and computed the electromagnetic transition rates. They are included in Table III together with the theoretical calculations by Jiang and coworkers and to the B($E2$) measurements by Diriken *et al.* [15] using the Coulomb excitation measurement of the ^{73}Ga $1/2^-$ ground state.

Given the $3/2^-$ spin-parity of the 217.4-keV level, the 217.4-keV de-exciting transition presumably feeds both the

FIG. 6. Extended level scheme of ^{73}Ga populated in the β^- decay of ^{73}Zn. New levels and γ-rays transitions are marked in red, while those in black were already seen in previous β-decay studies [21], apart from the 1979.9-keV transition, which was seen but not placed in the decay scheme. Dashed arrows indicate tentatively placed transitions.
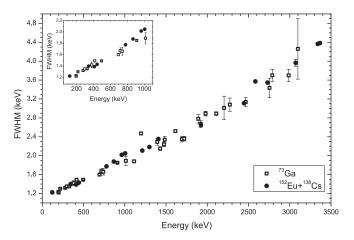
FIG. 7. Functional relation between peak widths and their energy. Circles indicate the trend for ^{152}Eu and ^{138}Cs calibration sources, only composed of single peaks, whereas squares present the relation for the γ rays present in the ^{73}Zn decay. The inset provides a closer look at the region from 0 to 1100 keV, where most of the transitions that most likely feed both states lay.

$1/2^-$–$3/2^-$ g.s. doublet. Both components may have an admixture of $M1$ and $E2$ multipoles, with the $M1$ component likely to be dominant. The $B(E2)$ and $B(M1)$ values calculated from the lifetime of 67 ± 9 ps assuming pure multipolarity (Table III) support a dominant $M1$ character and in fact a very small $E2$ decay branch ranging from 0.60% to 1.13% is required to match the B($E2$) = 7.2(10) W.u. from Coulomb excitation [15]. The B($M1$) transition rate of $4.5(6) \times 10^{-2}$ W.u. is in good agreement with the systematics [42] for this mass region. Our shell-model calculations point towards strongly mixed wave functions for the low-lying states and support a strong decay branch from the 217.4-keV level to the $1/2^-$ member of the ground-state doublet. The NPA calculations [41] also favor a major 217.4-keV branch feeding the $1/2^-$ ground state built on a $Dp_{3/2}$ configuration (where D stands for a proton pair coupled to 2^+ spin) while the $3/2^-$ member of the g.s. doublet has a dominant $p_{3/2}$ proton configuration. Regarding a possible $M1$ 19.0-keV transition connecting the 217.4- and 198.4-keV levels, its intensity would be below 0.1 units, beyond our
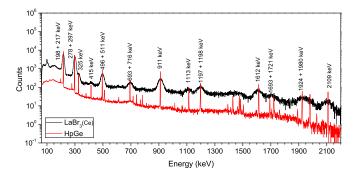

FIG. 8. A LaBr$_3$(Ce) energy spectrum with the most relevant peaks from the β decay of ^{73}Zn labeled. The spectrum is compared to the high-resolution HPGe one displayed in red. A detection condition on the β particles is set for both spectra.
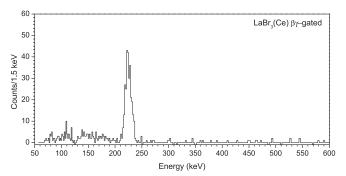

FIG. 9. Energy spectrum of the LaBr$_3$(Ce) detector with a detection condition on β particles and an energy gate set at the 693-keV γ ray on the HPGe detectors. A very clean peak at 217 keV is shown is the spectrum.

sensitivity, and furthermore at the low-energy detection threshold of the HPGe detectors (see Fig. 2).

For the second $3/2^-$ in the level scheme at 910.7 keV we could only set an upper limit for its lifetime, yielding lower bounds for the $M1$ transition rates that are consistent with the systematics. The relative transition rates for the three de-exciting transitions are very consistent, giving values within a factor of 2. We note that for the B($M1$) transition rates to be of the same order of magnitude than those de-exciting the 217.4-keV level ($\sim 4 \times 10^{-2}$ W.u.) the 910.7-keV mean-life should be below 1 ps.

Concerning the $5/2^-$ states at 198.4 and 495.6 keV, both are Coulomb excited in Ref. [15] and their de-exciting transitions appear Doppler-broadened, thus setting an upper limit on their lifetimes. For the 495.6-keV state we have measured a mean life of $\tau = 32(9)$ ps. The 495.6 keV de-exciting transition is expected to preferably feed the $3/2^-$ member of the g.s. doublet, with a dominant $M1$ multipolarity. This is
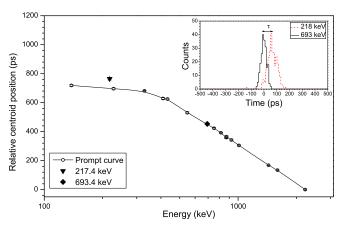

FIG. 10. Time response of the experimental setup for the full-energy peaks as a function of energy. The distribution is plotted from 100 to 2200 keV in logarithmic energy scale with hollow circles and a line to guide the eye. The triangle and the diamond indicate the centroid positions from the $\beta\gamma\gamma$ time-delayed spectrum at the energies of 217.4 and 693.4 keV, already corrected for Compton contribution. The 693.4 keV point is shifted to the calibration curve. The centroid shift for the 217.4 keV is given by the distance to the calibration curve and yields the 217.4 keV lifetime.

TABLE III. Half-lives of excited states in ^{73}Ga and experimental B($M1$) and B($E2$) reduced transition probabilities for the de-exciting transitions, assuming pure multipolarities. They are compared to the theoretical values obtained from the NPA model in Ref. [41] and to the B($E2$) values extracted from Coulomb excitation [15], when available. See text for details.

E_{level}^i	τ	J^π	E_γ	E_{level}^f	J^π	$B(M1) \times 10^{-2}$ (W.u.)			$B(E2)$ (W.u.)			
(keV)	(ps)		(keV)	(keV)		Exp.	NPA	jj44b	Exp.	NPA	jj44b	CoulEx
$\leqslant 0.3$		$3/2^-$	$\leqslant 0.3$	0.0	$1/2^-$		30.7	7.6		4.06	13.9	
198.4		$5/2^-$	198.4	0.0	$1/2^-$		—	—		17.2	12.3	11(2)
				$\leqslant 0.3$	$3/2^-$		0.5	0.07		2.07	0.2	
217.4	67(9)	$3/2^-$	217.4	0.0	$1/2^-$	4.6(7)	0.4	7.34	1330(18)[a]	20.0	14.0	7.5(10)
				$\leqslant 0.3$	$3/2^-$		94.1			1.62		
495.6	32(9)	$5/2^-$	495.6	0.0	$1/2^-$	—			44(12)[b]		10.3	6.5(10)
				$\leqslant 0.3$	$3/2^-$	0.75(21)		1.33			27.4	
			297.3	198.4	$5/2^-$	0.025(7)		1.31	4.0(11)		2.6	
			277.8	217.4	$3/2^-$	0.32(9)		1.53	58(16)		12.3	
910.7	$\leqslant 40$	$3/2^-$	910.6	0.0	$1/2^-$	$\geqslant 0.08$		2.17	$\geqslant 1.4$		0.2	
				$\leqslant 0.3$	$3/2^-$							
			693.4	217.4	$3/2^-$	$\geqslant 0.044$			$\geqslant 1.3$			
			415.2	495.6	$5/2^-$	$\geqslant 0.061$		23.6	$\geqslant 5.1$		6.2	

[a] An $E2$ branch ranging from 0.60% to 1.13% is required to match the $E2$ CoulEx value.

[b] A 15(4)% $E2$ branch needed to match the $E2$ CoulEx value, yielding $B(M1) = 5.6(16) \times 10^{-3}$ W.u.

supported by the shell-model calculations. From the Coulomb excitation value for the $E2$ transition to the g.s., B($E2; 5/2^- \rightarrow 1/2^-$) = 6.5(10) W.u. and the measured lifetime a branch of 15(4)% is obtained, where the $E2$ component of the $5/2^- \rightarrow 3/2^-$ transition has been neglected. The $M1$ branch amounts therefore to 85(4)%.

Due to the spin-parity of $5/2^-$ for the level at 198.4 keV, a similar pattern is expected, with a stretched $E2$ transition feeding the $1/2^-$ ground state, and a strong $M1$ component. Former studies [15] have shown that the 198.4-keV decay is a mixed transition feeding both the g.s. and the first-excited $3/2^-$ level, and this is also seen in the theoretical calculations [41]. If we assumed the same $E2$ branch of 15(4)% than for the 495.6-keV transition, the resulting level half-life that matches the CoulEx value of B($E2; 5/2^- \rightarrow 1/2^-$) = 7.5(10) W.u. would be $T_{1/2}^{198} = 2.0$ ns. Although the limited amount of statistics does not allow us to measure the state lifetime such a long value can be excluded from our fast-timing analysis. This is in line with the observation of a Doppler-broadened peak in Ref. [15]. Therefore, the lifetime should be much shorter, leading to an enhanced 198.4-keV $M1$ component with a preferred decay to the $3/2^-$ member of the ground state. This is in line with our shell model calculations, which yield a 93% branch to the $3/2^-$ level.

All the above confirms the spin-parity assignments for the low-lying levels in ^{73}Ga [10–12,15] and picture a different decay pattern to the $1/2^-$ or $3/2^-$ members of the g.s. doublet for γ cascades that transit through the 198.4- or 217.4-keV levels. Based on this we have attempted to measure the energy splitting of the g.s. doublet by using the energy differences of the γ cascades, as discussed in Sec. III.

V. CONCLUSIONS AND OUTLOOK

The low-lying structure of ^{73}Ga constitutes a special case in the nuclear chart, since it has a ground-state spin-parity of $1/2^-$ [6], in contrast with the systematics of the region, and a low-lying $3/2^-$ state with excitation energy below 1 keV [15]. In this work we took advantage of the purity and the large yield of the ^{73}Zn beam available at ISOLDE to extend the decay scheme of ^{73}Zn to ^{73}Ga and investigate the energy difference between the $1/2^-$ ground state and the $3/2^-$ first excited state. From the evaluation of the decay cascades and the peak width, we could set an upper limit for the energy splitting of 0.3 keV. In addition, we have extended the existing ^{73}Zn decay to ^{73}Ga with 8 new levels and 35 transitions not seen in previous β-decay studies [19,21]. The energies of several states previously observed in transfer reactions [10–12] have been more precisely determined. We have used the Advanced Time-Delayed method $\beta\gamma\gamma(t)$ method [23,24] to measure the lifetimes of the 217.4 keV $3/2_2^-$ state ($T_{1/2}^{217} = 47(6)$ ps) and the 495.6 keV $5/2_2^-$ state ($T_{1/2}^{496} = 22(6)$ ps), and to set a limit of $T_{1/2}^{911} \leqslant 28$ ps for the 910.7-keV $3/2_3^-$ level.

From the β-decay feeding and the reduced transition probabilities obtained from the measured level lifetimes, and the γ-decay branches, the observed structure of ^{73}Ga is consistent with the established spin-parity assignments at low energy. This is relatively well reproduced by the available theoretical calculations [20,41]. The measured 87(3)% ground state β feeding from the $(1/2^-)$ ^{73}Zn parent supports the $1/2^-$ assignment for the ground state of ^{73}Ga. We observed several β-fed states above 2 MeV, with likely $1/2^-$ or $3/2^-$ spins and parities, which had not been experimentally measured before.

The observation of a 195-keV transition is consistent with a γ-ray de-exciting a short-lived state in the β-decay parent ^{73}Zn, with a half-life in agreement with the reported value of $T_{1/2} = 13.0(2)$ ms in Ref. [20], but not with the earlier claim [19] of a β-decaying ^{73m}Zn isomeric state. It will be of interest to study the β decay of ^{73}Cu to ^{73}Zn to clarify the configuration of the 195-keV state and the presence of other isomeric states in the $A = 73$ chain.

Concerning the low-lying $3/2_1^-$ state in ^{73}Ga, alternative methods, such as selective ionization and decay, high-resolution mass spectrometry [43] or conversion electron detection after trapping [17], will be required to further investigate its nature and decay pattern.

[1] J. Van de Walle, F. Aksouh, T. Behrens, V. Bildstein, A. Blazhev, J. Cederkäll, E. Clément, T. E. Cocolios, T. Davinson, P. Delahaye, J. Eberth, A. Ekström, D. V. Fedorov, V. N. Fedosseev, L. M. Fraile, S. Franchoo, R. Gernhauser, G. Georgiev, D. Habs, K. Heyde, G. Huber, M. Huyse, F. Ibrahim, O. Ivanov, J. Iwanicki, J. Jolie, O. Kester, U. Köster, T. Kröll, R. Krücken, M. Lauer, A. F. Lisetskiy, R. Lutter, B. A. Marsh, P. Mayet, O. Niedermaier, M. Pantea, R. Raabe, P. Reiter, M. Sawicka, H. Scheit, G. Schrieder, D. Schwalm, M. Seliverstov, T. Sieber, G. Sletten, N. Smirnova, M. Stanoiu, I. Stefanescu, J.-C. Thomas, J. J. Valiente-Dobón, P. V. Duppen, D. Verney, D. Voulot, N. Warr, D. Weisshaar, F. Wenander, B. H. Wolf, and M. Zielińska, Phys. Rev. C **79**, 014309 (2009).

[2] R. Orlandi, D. Mücher, R. Raabe, A. Jungclaus, S. Pain, V. Bildstein, R. Chapman, G. de Angelis, J. Johansen, P. V. Duppen, A. Andreyev, S. Bottoni, T. Cocolios, H. D. Witte, J. Diriken, J. Elseviers, F. Flavigny, L. Gaffney, R. Gernhäuser, A. Gottardo, M. Huyse, A. Illana, J. Konki, T. Kröll, R. Krücken, J. Lane, V. Liberati, B. Marsh, K. Nowak, F. Nowacki, J. Pakarinen, E. Rapisarda, F. Recchia, P. Reiter, T. Roger, E. Sahin, M. Seidlitz, K. Sieja, J. Smith, J. V. Dobón, M. von Schmid, D. Voulot, N. Warr, F. Wenander, and K. Wimmer, Phys. Lett. B **740**, 298 (2015).

[3] X. F. Yang, C. Wraith, L. Xie, C. Babcock, J. Billowes, M. L. Bissell, K. Blaum, B. Cheal, K. T. Flanagan, R. F. Garcia Ruiz, W. Gins, C. Gorges, L. K. Grob, H. Heylen, S. Kaufmann, M. Kowalska, J. Kraemer, S. Malbrunot-Ettenauer, R. Neugart, G. Neyens, W. Nörtershäuser, J. Papuga, R. Sánchez, and D. T. Yordanov, Phys. Rev. Lett. **116**, 182502 (2016).

[4] A. Gottardo, D. Verney, C. Delafosse, F. Ibrahim, B. Roussière, C. Sotty, S. Roccia, C. Andreoiu, C. Costache, M.-C. Delattre, I. Deloncle, A. Etilé, S. Franchoo, C. Gaulard, J. Guillot, M. Lebois, M. MacCormick, N. Marginean, R. Marginean, I. Matea, C. Mihai, I. Mitu, L. Olivier, C. Portail, L. Qi, L. Stan, D. Testov, J. Wilson, and D. T. Yordanov, Phys. Rev. Lett. **116**, 182501 (2016).

[5] S. Suchyta, S. N. Liddick, Y. Tsunoda, T. Otsuka, M. B. Bennett, A. Chemey, M. Honma, N. Larson, C. J. Prokop, S. J. Quinn, N. Shimizu, A. Simon, A. Spyrou, V. Tripathi, Y. Utsuno, and J. M. VonMoss, Phys. Rev. C **89**, 021301 (2014).

[6] B. Cheal, E. Mané, J. Billowes, M. L. Bissell, K. Blaum, B. A. Brown, F. C. Charlwood, K. T. Flanagan, D. H. Forest, C. Geppert, M. Honma, A. Jokinen, M. Kowalska, A. Krieger, J. Krämer, I. D. Moore, R. Neugart, G. Neyens, W. Nörtershäuser, M. Schug, H. H. Stroke, P. Vingerhoets, D. T. Yordanov, and M. Žáková, Phys. Rev. Lett. **104**, 252502 (2010).

[7] C. Louchart, A. Obertelli, A. Görgen, W. Korten, D. Bazzacco, B. Birkenbach, B. Bruyneel, E. Clément, P. J. Coleman-Smith, L. Corradi, D. Curien, G. de Angelis, G. de France, J.-P. Delaroche, A. Dewald, F. Didierjean, M. Doncel, G. Duchêne, J. Eberth, M. N. Erduran, E. Farnea, C. Finck, E. Fioretto, C. Fransen, A. Gadea, M. Girod, A. Gottardo, J. Grebosz, T. Habermann, M. Hackstein, T. Huyuk, J. Jolie, D. Judson, A. Jungclaus, N. Karkour, S. Klupp, R. Krücken, A. Kusoglu, S. M. Lenzi, J. Libert, J. Ljungvall, S. Lunardi, G. Maron, R. Menegazzo, D. Mengoni, C. Michelagnoli, B. Million, P. Molini, O. Möller, G. Montagnoli, D. Montanari, D. R. Napoli, R. Orlandi, G. Pollarolo, A. Prieto, A. Pullia, B. Quintana, F. Recchia, P. Reiter, D. Rosso, R. Wother, E. Sahin, M.-D. Salsac, F. Scarlassara, M. Schlarb, S. Siem, P. P. Singh, P.-A. Söderström, A. M. Stefanini, O. Stézowski, B. Sulignano, S. Szilner, C. Theisen, C. A. Ur, J. J. Valiente-Dobón, and M. Zielinska, Phys. Rev. C **87**, 054302 (2013).

[8] G. Gürdal, E. A. Stefanova, P. Boutachkov, D. A. Torres, G. J. Kumbartzki, N. Benczer-Koller, Y. Y. Sharon, L. Zamick, S. J. Q. Robinson, T. Ahn, V. Anagnostatou, C. Bernards, M. Elvers, A. Heinz, G. Ilie, D. Radeck, D. Savran, V. Werner, and E. Williams, Phys. Rev. C **88**, 014301 (2013).

[9] B. Pritychenko, J. Choquette, M. Horoi, B. Karamy, and B. Singh, At. Data Nucl. Data Tables **98**, 798 (2012).

[10] M. N. Vergnes, G. Rotbard, E. R. Flynn, D. L. Hanson, S. D. Orbesen, F. Guilbault, D. Ardouin, and C. Lebrun, Phys. Rev. C **19**, 1276 (1979).

[11] G. Rotbard, M. Vergnes, G. Berrier-Ronsin, and J. Vernotte, Phys. Rev. C **21**, 2293 (1980).

[12] G. Rotbard, G. LaRana, M. Vergnes, G. Berrier, J. Kalifa, F. Guilbault, and R. Tamisier, Phys. Rev. C **18**, 86 (1978).

[13] J. Neijzen and A. Dönszelmann, Physica B+C **98**, 235 (1980).

[14] I. Stefanescu, W. B. Walters, R. V. F. Janssens, S. Zhu, R. Broda, M. P. Carpenter, C. J. Chiara, B. Fornal, B. P. Kay, F. G. Kondev, W. Krolas, T. Lauritsen, C. J. Lister, E. A. McCutchan, T. Pawlat, D. Seweryniak, J. R. Stone, N. J. Stone, and J. Wrzesinski, Phys. Rev. C **79**, 064302 (2009).

[15] J. Diriken, I. Stefanescu, D. Balabanski, N. Blasi, A. Blazhev, N. Bree, J. Cederkäll, T. E. Cocolios, T. Davinson, J. Eberth, A. Ekström, D. Fedorov, V. Fedosseev, L. Fraile, S. Franchoo, G. Georgiev, K. Gladnishki, M. Huyse, O. V. Ivanov, V. S. Ivanov,

J. Iwanicki, J. Jolie, T. Konstantinopoulos, T. Kröll, R. Krücken, U. Köster, A. Lagoyannis, G. Lo Bianco, P. Maierbeck, B. A. Marsh, P. Napiorkowski, N. Patronis, D. Pauwels, P. Reiter, M. Seliverstov, G. Sletten, J. Van de Walle, P. Van Duppen, D. Voulot, W. B. Walters, N. Warr, F. Wenander, and K. Wrzosek, Phys. Rev. C **82**, 064309 (2010).

[16] B. R. Beck, J. A. Becker, P. Beiersdorfer, G. V. Brown, K. J. Moody, J. B. Wilhelmy, F. S. Porter, C. A. Kilbourne, and R. L. Kelley, Phys. Rev. Lett. **98**, 142501 (2007).

[17] L. von der Wense, B. Seiferle, M. Laatiaoui, J. B. Neumayr, H.-J. Maier, H.-F. Wirth, C. Mokry, J. Runke, K. Eberhardt, C. E. Düllmann *et al.*, Nature **533**, 47 (2016).

[18] E. Browne and J. Tuli, Nucl. Data Sheets **122**, 205 (2014).

[19] E. Runte *et al.*, Nucl. Phys. A **441**, 237 (1985).

[20] M. Huhta, P. F. Mantica, D. W. Anthony, P. A. Lofy, J. I. Prisciandaro, R. M. Ronningen, M. Steiner, and W. B. Walters, Phys. Rev. C **58**, 3187 (1998).

[21] E. Runte *et al.*, Nucl. Phys. A **399**, 163 (1983).

[22] B. Singh, Nucl. Data Sheets **101**, 193 (2004).

[23] H. Mach, R. Gill, and M. Moszyński, Nucl. Instrum. Methods Phys. Res., Sect. A **280**, 49 (1989).

[24] M. Moszyński and H. Mach, Nucl. Instrum. Methods Phys. Res., Sect. A **277**, 407 (1989).

[25] http://isolde.web.cern.ch/is441.

[26] R. Lica, N. Marginean, D. G. Ghiţa, H. Mach, L. M. Fraile, G. S. Simpson, A. Aprahamian, C. Bernards, J. A. Briz, B. Bucher, C. J. Chiara, Z. Dlouhý, I. Gheorghe, P. Hoff, J. Jolie, U. Köster, W. Kurcewicz, R. Marginean, B. Olaizola, V. Paziy, J. M. Régis, M. Rudigier, T. Sava, M. Stanoiu, L. Stroe, and W. B. Walters, Phys. Rev. C **90**, 014320 (2014).

[27] V. Paziy, L. M. Fraile, H. Mach, A. Aprahamian, C. Bernards, J. A. Briz, B. Bucher, C. J. Chiara, Z. Dlouhý, I. Gheorghe, D. G. Ghiţa, P. Hoff, J. Jolie, U. Köster, W. Kurcewicz, N. Marginean, R. Marginean, B. Olaizola, J. M. Régis, M. Rudigier, T. Sava, G. S. Simpson, M. Stanoiu, L. Stroe, and W. B. Walters, (unpublished).

[28] A. Gottberg, T. Mendonca, R. Luis, J. Ramos, C. Seiffert, S. Cimmino, S. Marzari, B. Crepieux, V. Manea, R. Wolf, F. Wienholtz, S. Kreim, V. Fedosseev, B. Marsh, S. Rothe, P. Vaz,

J. Marques, and T. Stora, Nucl. Instrum. Methods B **336**, 143 (2014).

[29] U. Köster, T. Behrens, C. Clausen, P. Delahaye, V. Fedoseyev, L. Fraile, R. Gernhäuser, T. J. Giles, A. Ionan, T. Kröll, H. Mach, B. Marsh, M. Seliverstov, T. Sieber, E. Siesling, E. Tengborn, F. Wenander, and J. Van de Walle, AIP Conf. Proc. **798**, 315 (2005).

[30] U. Köster, O. Arndt, E. Bouquerel, V. Fedoseyev, H. Frånberg, A. Joinet, C. Jost, I. Kerkines, and R. Kirchner, Nucl. Instrum. Methods Phys. Res., Sect. B **266**, 4229 (2008).

[31] V. N. Fedosseev, L.-E. Berg, D. V. Fedorov, D. Fink, O. J. Launila, R. Losito, B. A. Marsh, R. E. Rossel, S. Rothe, M. D. Seliverstov, A. M. Sjödin, and K. D. A. Wendt, Rev. Sci. Instrum. **83**, 02A903 (2012).

[32] X. LLC, "User's Manual Digital Gamma Finder (DGF) Pixie-4" (2009).

[33] A. Sonzogni, Nucl. Data Sheets **98**, 515 (2003).

[34] N. Nica, Nucl. Data Sheets **108**, 1287 (2007).

[35] National Nuclear Data Center. Retrieved from https://www.nndc.bnl.gov/.

[36] H. Mach, F. Wohn, G. Molnár, K. Sistemich, J. C. Hill, M. Moszyński, R. Gill, W. Krips, and D. Brenner, Nucl. Phys. A **523**, 197 (1991).

[37] B. Olaizola, L. M. Fraile, H. Mach, A. Aprahamian, J. A. Briz, J. Cal-González, D. Ghiţa, U. Köster, W. Kurcewicz, S. R. Lesher, D. Pauwels, E. Picado, A. Poves, D. Radulov, G. S. Simpson, and J. M. Udías, Phys. Rev. C **88**, 044306 (2013).

[38] J. Lettry, R. Catherall, P. Drumm, P. V. Duppen, A. Evensen, G. Focker, A. Jokinen, O. Jonsson, E. Kugler, and H. Ravn, Nucl. Instrum. Methods Phys. Res., Sect. B **126**, 130 (1997).

[39] P. C. Srivastava, J. Phys. G: Nucl. Part. Phys. **39**, 015102 (2012).

[40] A. Negret and B. Singh, Nucl. Data Sheets **114**, 841 (2013).

[41] H. Jiang, G. J. Fu, Y. M. Zhao, and A. Arima, Phys. Rev. C **84**, 034302 (2011).

[42] P. Endt, At. Data Nucl. Data Tables **23**, 547 (1979).

[43] W. R. Plaß, T. Dickel, and C. Scheidenberger, Int. J. Mass Spectrom. **349–350**, 134 (2013).